energies

MDPI

Article

Assessing the Economic Impact of Introducing Localised PV Solar Energy Generation and Energy Storage for Fleet Electrification

Maria Nunez Munoz [1,2], Erica E. F. Ballantyne [1] and David A. Stone [2,*]

[1] Sheffield University Management School, The University of Sheffield, Conduit Road, Sheffield S10 1FL, UK
[2] Department of Electronic and Electrical Engineering, The University of Sheffield, Sir Frederick Mappin Building, Mappin Street, Sheffield S1 3JD, UK
* Correspondence: d.a.stone@sheffield.ac.uk; Tel.: +44-114-2225046

Abstract: Greenhouse gas (GHG) emissions from the transport sector and their effect on air quality are now a major concern, and the electrification of road freight transport is seen as one potential solution. However, this presents a challenge with the increased electricity demand on a depot's grid connection, and increased costs if this has to be upgraded. This study seeks to evaluate the impact on costs of introducing solar (PV) panels and a Battery Energy Storage System (BESS) when a company electrifies its fleet, based on two different priorities. On one hand, avoiding the use of the grid at peak price periods at the expense of upgrading the power connection. On the other hand, avoiding any power connection upgrade at the expense of incurring excess capacity charges. These two priorities aim to represent real-life challenges that logistics and commercial companies are facing when it comes to fleet electrification. The choice of prioritising one over the other may be driven by operational requirements and/or technical constraints. For each approach, a different energy management algorithm is developed using MATLAB and Simulink. The results obtained suggest that there is more flexibility in cost reduction when the upgrade of the power connection is not an obstacle. If the upgrade of the power network is not an option, the installation of PV panels and a BESS must be implemented together with other strategies (i.e., smart charging) to make it an economic option.

Keywords: Battery Energy Storage System; localised solar energy generation; electric refuse collection fleet; energy management; road freight transport; decarbonisation; power network upgrade; system cost analysis

Citation: Munoz, M.N.; Ballantyne, E.E.F.; Stone, D.A. Assessing the Economic Impact of Introducing Localised PV Solar Energy Generation and Energy Storage for Fleet Electrification. *Energies* **2023**, *16*, 3570. https://doi.org/10.3390/en16083570

Academic Editor: Abdul-Ghani Olabi

Received: 27 February 2023
Revised: 6 April 2023
Accepted: 17 April 2023
Published: 20 April 2023

1. Introduction

Global efforts are focused on lowering the dependency on fossil fuels and reducing the carbon emissions. This is especially relevant within the transport sector. In the UK, transport is the largest emitting sector, responsible for 24% of the UK's total emissions [1]. Within this sector, road freight transport plays an important role not only due to its greenhouse gas (GHG) emissions but also because of its negative impact on air quality. Heavy goods vehicles (HGVs) and light goods vehicles (LGVs) are estimated to account for around 46% of total road transport NOx emissions [1], while making up just 6% and 18% of vehicle miles, respectively [1]. As a result, the road freight transport sector is the main target of policies such as Clean Air Zones (CAZ) and Low Emission Zones (LEZ) that local governments are implementing in major UK cities. CAZ and LEZ policies encourage the adoption of lower-emission vehicles by imposing a fee on those vehicles not meeting the set emission standards.

The electrification of a vehicle fleet, ideally powered by renewable energies [2], is seen as one potential solution. In particular, urban logistics, local authority fleets (i.e., waste management) or public transport fleets (i.e., bus fleets) can benefit the most from electrification within the road transport sector due to their well-structured and planned

daily routes [3–5]. Although there is no official number, there are some councils that have already replaced part of their fleet or are in trials to switch from conventional diesel power to electric. To name a few, in the UK there are some electric refuse collection vehicles (eRCVs) operating in London, Manchester, Brighton, York, Bournemouth, and Glasgow.

However, the electrification of the road freight transport sector is a challenge [6,7]. Transport operators' concerns focus on how to adapt their operations to EV fleets. According to experts in the field of urban freight transport and logistics [8], and transport electrification [9], charging infrastructure is presented as a large barrier for logistics and commercial companies. In fact, the implementation of charging points in commercial sites is still far behind expectations considering the positive outcome it entails for the commercial sector. The reality is that there are still significant barriers to this occurring [6]. Generally, the lack of charging infrastructure availability is a disincentive for the uptake of EVs [10,11]. Amazon exemplified this when its Director of Global Fleet and Products emphasised that EV charging infrastructure is one of the most challenging factors of decarbonisation strategy [12], with reference to its commitment to making 50% of all shipments net zero carbon by 2030 [13]. Likewise, the capital investment required [9], especially when current grid power connections do not meet potential EV fleet charging demand [14] during the off-hours at the depot [15], leading to companies being required to upgrade the utility grid connection [8,16] to ensure the demand is met [17].

Different authors have highlighted the power connection issue when the fleet is electrified. Pietracho et al. [17] assess the impact of the integration of EVs into the commercial sector, considering both economic and environmental factors when compared to conventional fleets. The authors concluded that the total cost of ownership (TCO) of electric fleets was higher when compared to conventional fleets due to the additional infrastructure costs of the charging stations.

Schmidt et al., [18] explored this topic by considering both the technical limitations of the vehicles (e.g., range) and the charging infrastructure (e.g., charging power and the number of charging stations). The study's aim was to inform on which fleet mobility patterns could benefit from adapting vehicle recharging strategies such that the outcome could be generalised to a wider range of commercial fleets. However, despite the study's valuable outcomes, it presents some limitations. With regard to the power connection, the author's strategy was to use the minimum required power capacity capable of ensuring uninterrupted operation. This is possible when, due to the reduced battery capacity of the vehicles studied (i.e., 40 kWh), the fleet can be charged during the night using an 11 kW charger. The results of the study can only be applied therefore to certain commercial services (i.e., those that require the use of light commercial vehicles), but when it comes to heavy vehicles with higher battery capacities (e.g., those used for waste management), the power required from the grid to recharge all of the vehicles would be considerably higher, and the outcomes obtained from this study are not applicable.

Kin et al. [19] discussed the techno-operational and financial feasibility of fleet electrification for a wider variety of commercial vehicles, one example quoted being small trucks with a battery capacity of 200 kWh. Due to the nature of this study being focused on discussing the outcomes from a case study, technicalities regarding power connections are not provided. However, the authors did highlight the power connection capacity issues at the local grid when heavy-duty vehicles (HGVs) are charged in a depot.

Pelletier et al. [20] explored the EV fleet charging strategies from a more technical perspective. The maximum power retrieved from the grid to charge the vehicles was one of the constraints of this study. Two maximum charging powers were studied, 20 kW and 500 kW. Results from this study suggest that when implementing power grid constraints, fleet charging becomes an unfeasible solution for one of the scenarios. The authors also concluded that limiting the power grid capacity may significantly increase energy costs under certain situations.

The research studies completed by Pelletier et al. [20], Schmidt et al. [18], or Kin, et al. [19], advised of the consequences or implications that a limitation on power grid connection

would have when it comes to electrifying a fleet, which is, unfortunately, a commonly encountered issue.

Some of the solutions to this problem explored in the literature have focused on smart charging [14] or load management [21,22]. These services and implementations have been the subject of research for many years [23,24], with both solutions complementing each other. Smart charging includes load management algorithms that flatten the load profile through coordinating vehicle charging [5]. Indirectly, when these approaches are applied, the cost of charging is reduced [25,26]. Both approaches are widely agreed to be vital elements of reducing costs when adopting electric fleets.

A complementary solution is energy storage. Energy storage has been shown to be a potential technology to facilitate the integration of EV fleets, particularly if the system is powered by renewable generation [27]. The potential benefits of integrating energy storage and renewable energy generation are highly dependent on the energy management strategy in the system. Energy management has been broadly studied by researchers from different viewpoints; to achieve better efficiency within a distribution network (i.e., loss minimization in the distribution systems) [28,29], to reduce costs by controlling the energy sources and controllable loads, or to reduce greenhouse gas (GHG) emissions [30,31]. Betz and Lienkamp [32] developed an energy management system to investigate the potential benefits of adopting EV fleets in commercial situations. The authors sought to efficiently integrate the three technologies (i.e., PV generation, energy storage, and EV fleets) to reduce total costs of ownership (TCO) and CO_2 emissions. When running their simulations, authors assumed the EV was available at the commercial site and could be used as a battery to store PV-generated surplus solar energy, avoiding the need of selling it back to the grid, indirectly increasing the self-consumption of PV solar energy.

Engelhardt et al. [33] developed a heuristic energy management system to allocate battery strings to other system components and to manage the energy exchange between a PV system, two EV fast chargers, and the grid. Arfeen et al. [34] developed a rule-based energy management algorithm for EV rapid charging considering a PV system and battery storage.

Despite the number of research publications focused on commercial fleet electrification or the development of energy management algorithms to integrate EVs and renewable energies, the authors of this study have identified a gap in the literature that links both topics. In this study, authors seek to evaluate the impacts on costs when a company electrifies the fleet using PV generation and a BESS. For this study, battery degradation [35,36] has not been considered as part of the economic analysis; however, due to its relevance on costs, battery degradation is being considered as part of future research.

The economic analysis is performed based on two different priorities: On one hand, avoiding the use of the grid during peak price periods, at the expense of upgrading the grid power connection; On the other hand, avoiding any power connection upgrade at the expense of possibly incurring excess capacity charges. These two priorities aim to represent the real-life challenges that logistics and commercial companies are facing when it comes to introducing fleet electrification. The choice of prioritising one over the other is subject to operational requirements and/or technical constraints at each individual location.

To facilitate the analysis of these scenarios, a rule-based energy management algorithm has been developed [34,37] for each priority set previously. Both algorithms are in the form of "if"/"else" and "then" statements. Ruled-based control strategy algorithms benefit from being simple to integrate [38] and have been successfully applied to PV+ BESS systems previously by other authors [34,37,39].

Three objectives have been set to meet the aim of this study:

1. To evaluate the economic benefits, if any, of introducing a PV installation and a BESS on site when a Waste Management Depot (WMD) adopts a fleet of eRCVs. For that purpose, the costs associated with the scenarios are compared.
2. To determine which of the two strategies simulated in this study, employing a PV installation and a BESS on site, report better economic benefits.

3. To create a set of conclusions that contribute to the technical and economic knowledge of the electrification of road freight and transportation.

The remainder of this paper is structured as follows: firstly, a description of the methodology adopted is introduced. The PV solar model used to estimate solar energy generation is described and the energy management algorithms used are introduced. At the end of the section, a description of the system cost analysis is also included. Following this, the results are analysed and evaluated according to each objective. The findings and conclusions are summarized at the end of the paper.

2. Methodology

2.1. Description of the Building under Study

In this study, a local authority waste management depot (WMD) in Nottinghamshire, UK, has been examined. The site includes two different buildings, with floor areas of 2445 m^2 and 2361 m^2, respectively. The local authority provided hourly energy consumption data from 1 April 2021 to 31 March 2022. The total energy consumption for both buildings was 234 MWh for this period, with a peak demand of 102 kWh. The energy intensity for the WMD is approximately 49 kWh/m^2. For the purpose of this study, it is assumed that the WMD would switch its fleet of refuse collection vehicles (RCVs) from conventional to electric drive.

Next, details regarding the fleet are introduced.

2.2. WMD Fleet Operational Times and Charging Pattern

The current WMD refuse collection vehicle (RCV) fleet comprises 19 diesel RCVs, with a total monthly distance travelled and fuel consumed of approximately 23,000 miles and 19,500 litres, respectively.

It is assumed that the entire RCV fleet is to be switched from diesel to electric, and as the mileage of the conventional RCV fleet is available, a conversion factor was used (3.48 kWh/mile) to calculate the total energy requirement of the existing fleet. The conversion factor was obtained from an energy consumption model for eRCVs proposed by [40]. The battery capacity of each eRCV is assumed to be 300 kWh, based on the average battery size of several eRCV manufacturers' prototypes.

Each eRCV has its own 22 kW charger and is charged at the depot. The model assumes that the fleet operates Monday to Friday with a constant daily consumption of 185 kWh. The eRCV fleet will operate between 06:00 h and 14:00 h and will return to the depot to be charged from 21:00 h for a maximum of 8.5 h, thus, the vehicles depart from the depot with a fully charged battery. This operating schedule is commensurate with the existing diesel fleet operation.

Switching the RCV fleet from diesel to electric increases the energy demand of the depot site. Precisely, the total demand for the WMD would increase from 234 MWh to 914 MWh per year (as shown later).

2.3. Scenarios

Three different scenarios have been considered to evaluate the impact of having PV panels and a BESS installed on-site, shown diagrammatically in Figure 1.

Scenario 1 (Figure 1a) assumes that the company does not have PV panels, nor a BESS installed and that the site is fully dependent on the grid connection to cover both the existing depot load and the eRCV fleet energy demand.

Scenario 2 (Figure 1b) considers that the WMD has PV panels and a BESS installed. Both the depot and the eRCV fleet energy demands are covered by using energy from the grid and from the PV solar installation. The energy flow for scenario 2 is controlled throughout by an algorithm that is set to avoid the use of the grid during peak price periods, at the expense of upgrading the grid power connection. Due to the increase in energy demand after the introduction of the eRCV fleet, the grid power connection capacity is

assumed to be upgraded from 0.15 MW to 0.6 MW. A detailed description of the algorithm is included in Section 2.5.1.

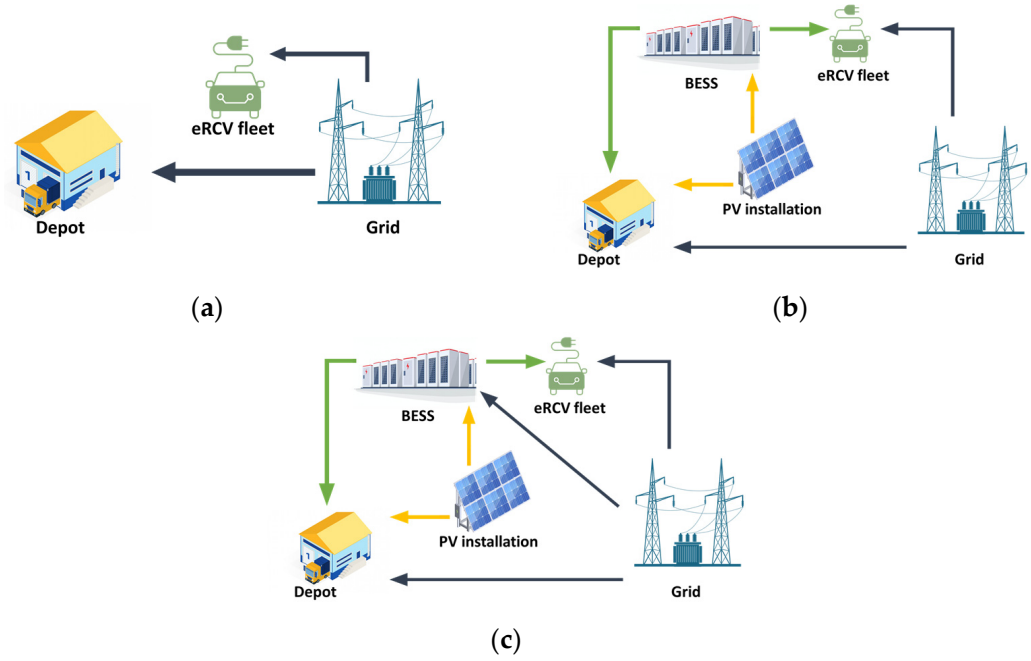

Figure 1. Energy flow diagram for (**a**) scenario 1, (**b**) scenario 2 and, (**c**) scenario 3.

Scenario 3 (Figure 1c) has PV panels and a BESS installed at the WMD as in scenario 2; however, the BESS in this scenario is not only charged from the PV solar installation but also from the grid. As in scenario 2, an algorithm has been developed to manage to energy flow. The objective of the algorithm is to avoid any grid power connection upgrade despite the increase in energy demand after introducing the eRCV fleet into the WMD at the expense of using the grid-supplied energy at peak prices. Therefore, the power capacity connection remains at 0.15 MW. Details about the algorithm created for scenario 3 are explained in Section 2.5.2.

With the objective of facilitating an economic comparison between the three scenarios, the analysis for scenario 1 is performed using both power connection capacities, 0.15 MW and 0.6 MW. Table 1 summarises the scenarios studied, and the power connection capacity assumed for each.

Table 1. Summarise of the scenarios under study and the approach used for the costs analysis.

	Power Connection Capacity (0.15 MW)	Power Connection Capacity (0.6 MW)
Scenario 1	✓	✓
Scenario 2		✓
Scenario 3	✓	

Next, the solar model used to estimate the solar energy generation at the WMD for scenario 2 and scenario 3 is explained.

2.4. Estimation of PV Solar Energy Generation

The PV energy generation for scenario 2 and scenario 3 was modelled using MATLAB, following the steps shown in Figure 2. The hourly solar irradiation data for this study was obtained through the Centre for Environmental Data Analysis (CEDA) archive. The CEDA archive is the UK national data centre for atmospheric and earth observation research that ensures easy access to horizontal solar irradiation data from the open data version of the Met Office Integrated Data Archive System (MIDAS) [41,42]. The hourly data was

measured at a weather station located in Walnatt (Nottinghamshire, UK) between 2009 and 2019 in kJ/m^2. The values of global solar irradiation were then averaged and transformed into kWh/m^2 to be used as input to the solar model. The datasets correspond to hourly measurements of horizontal global solar irradiation (G_H). Empirical correlations were used to estimate values of horizontal diffuse solar radiation ($G_{d,est}$) [43].

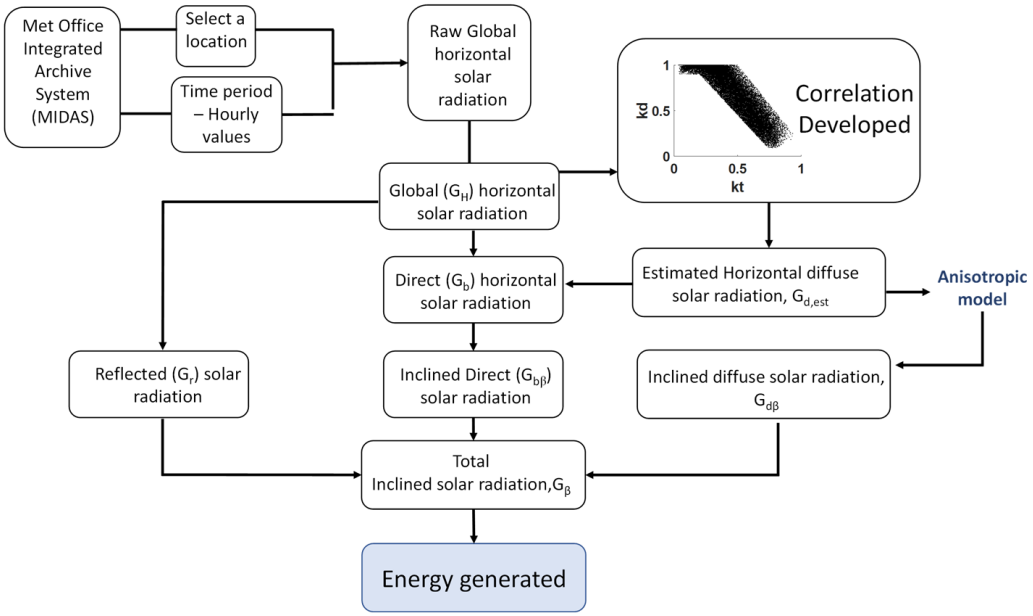

Figure 2. Diagram followed for the estimation of PV solar energy.

Once the global and diffuse horizontal solar radiation values are known, the direct horizontal radiation (G_b) can be accurately calculated. Equation (1) is

$$G_b\left[\frac{kWh}{m^2}\right] = G_H - G_{d,est} \quad (1)$$

The direct irradiation on inclined surfaces ($G_{b\beta}$) can be computed using geometrical relationships (i.e., angle of incidence and zenith angle) between the horizontal and inclined surfaces, following Equation (2):

$$G_{b\beta}\left[\frac{kWh}{m^2}\right] = \frac{G_b}{\sin(\gamma_s)} \cdot \cos(\theta). \quad (2)$$

γ_s is the solar altitude and θ is the solar incidence angle. The equations to calculate both parameters are presented as Equations (3) and (4), respectively.

$$\gamma_s = \text{asin}(\sin\varphi \cdot \sin\delta - \cos\varphi \cdot \cos\delta \cdot \cos\omega)\ [\text{degrees}], \quad (3)$$

$$\cos\theta = (\cos\gamma_s \cdot \cos(\alpha_S - \alpha) \cdot \sin\beta) + (\cos\beta \cdot \sin\gamma_s)\ [\text{degrees}], \quad (4)$$

where φ is the latitude, δ is the declination angle (Equation (5)), α_S is the solar azimuth (Equation (6)), α is the angle at which the panel is orientated, ω is the hour angle (Equation (7)), and β is the tilt angle of the PV panels. For the WMD PV installation, the PV panels are assumed to be tilted at the existing roof inclination angle, 30 degrees and orientated towards the southeast (140 degrees) and the northwest (320 degrees).

$$\delta = 23.45 \cdot \sin\left[360 \cdot \frac{(DOY + 284)}{365}\right][\text{degrees}]. \quad (5)$$

DOY is the day-of-year, and it represents the n^{th} day of the year (i.e., 1 January is DOY = 1; 1 February is DOY = 32, 1 March is DOY = 60, etc. Leap year is not included).

The azimuth angle calculation follows the equations below [44,45].

$$\begin{array}{l}\text{For morning hours, } t \leq 12\\ \qquad \text{For } \omega \leq 180,\ \cos\alpha_s = \left(\frac{\sin\ \delta\cdot\cos\ \varphi\ +\ \sin\ \varphi\cdot\cos\ \delta\cdot\cos\ \omega}{\cos\ \gamma_S}\right)\\ \text{The afternoon azimuth, for } t > 12\\ \qquad \text{For } \omega > 180,\ \cos\alpha_s = 360 - \left(\frac{\sin\ \delta\cdot\cos\ \varphi\ +\ \sin\ \varphi\cdot\cos\ \delta\cdot\cos\ \omega}{\cos\ \gamma_S}\right),\end{array} \tag{6}$$

$$\omega = t\cdot 15^{\circ}[\text{degrees}] \tag{7}$$

t is local solar time. From [46], the standard time used for the UK observations is Universal Time Coordinated (UTC) and daylight savings are not considered. Accordingly, t is estimated following Brownson et al. [47] as in Equation (8);

$$t = LMT + \frac{\lambda - \lambda_R}{15} + EOT\ [\text{hours}], \tag{8}$$

where LMT is the local mean time or civil time. λ is the longitude of the standard time meridian, λ_R is the longitude of the location, and EOT is the equation of time [48]. EOT can be estimated following Equation (9).

$$EOT = 229.2\cdot(0.000075 + 0.001868\cdot\cos B - 0.032077\cdot\sin B - 0.014615\cdot\cos 2B - 0.04089\cdot\sin\ 2B)[\text{minutes}] \tag{9}$$

where B is a coefficient calculated by Duffie et al. [48], following Equation (10).

$$B = (DOY - 1)\cdot\frac{360}{365}. \tag{10}$$

However, it is not possible to calculate diffuse irradiation on inclined surfaces ($G_{d\beta}$) using a geometrical relationship as the diffuse component comes from all points of the sky [49,50]. For this study, Reindl's anisotropic model [51] has been used to estimate $G_{d\beta}$ (Equation (11)).

$$G_{d\beta}[\frac{kWh}{m^2}] = G_d\cdot\left[F_{Hay}\cdot\frac{\cos(\theta)}{\sin(\gamma_s)} + (1 - F_{Hay})(\frac{1+\cos\beta}{2})(1 + f_R\sin^3(\frac{\beta}{2}))\right], \tag{11}$$

where F_{Hay} (Equation (12)) is an anisotropic index and f_R is the modulating function (Equation (13)) that accounts for the impact of an overcast sky on diffuse radiation intensity:

$$F_{Hay} = \frac{G_b}{G} \tag{12}$$

G is the hourly horizontal extra-atmospheric irradiance.

$$f_R = \sqrt{\frac{G_b}{G_H}} \tag{13}$$

The reflected irradiation (G_r) can be obtained knowing G_H and the albedo (ρ) using Equation (14). The albedo is the reflectance of the ground for solar radiation. The surface material assumed for the purpose of this study is concrete, with an albedo value of 0.2.

$$G_r[\frac{kWh}{m^2}] = G_H\cdot\rho\cdot(\frac{1-\cos\beta}{2}). \tag{14}$$

The total inclined solar radiation (G_β) can be calculated as the addition of the beam component from direct inclined radiation ($G_{b\beta}$), diffuse inclined radiation ($G_{d\beta}$), and reflected radiation (G_r) (Equation (15)).

$$G_\beta\left[\frac{\text{kWh}}{\text{m}^2}\right] = G_{b\beta} + G_{d\beta} + G_r. \quad (15)$$

The solar model predicts solar irradiation received on an inclined surface. However, the most interesting parameter for the implementation of the solar generation system is energy generation. Thus, the model developed transformed the solar irradiation calculated into energy generation by considering inverter efficiency (ηi), panel efficiency (ηp), and panel dimensions and a total number of panels following Equation (16).

$$\text{Energy generated [kWh]} = G_\beta\left(\frac{\text{kWh}}{\text{m}^2}\right)\cdot\eta\text{i}\cdot\eta\text{p}\cdot\text{panel dimensions}\left(\text{m}^2\right)\cdot\text{n}^\circ\text{of panels}. \quad (16)$$

It has been assumed that the PV installation has 946 PV panels on one of the buildings and 918 PV panels on the other, commensurate with the available roof sizes of the existing depot buildings. The area of the chosen PV panels is 1.64 m^2, inverter efficiency (ηi) and panel efficiency (ηp) are assumed to be 80% and 14%, respectively. From this arrangement, the modelled total PV energy generation from April 2021 until the end of March 2022 was 328 MWh.

The modelled PV solar energy generation at the WMD can be seen in Figure 3 (yellow column) as a comparison with the WMD energy consumption (orange column) when the WMD has a fleet of conventional diesel RCVs (Figure 3a), and when the fleet is switched to eRCVs (Figure 3b). As it was previously mentioned, replacing a diesel-powered fleet of RCVs with an electric fleet has a significant impact on the energy demand required at the site.

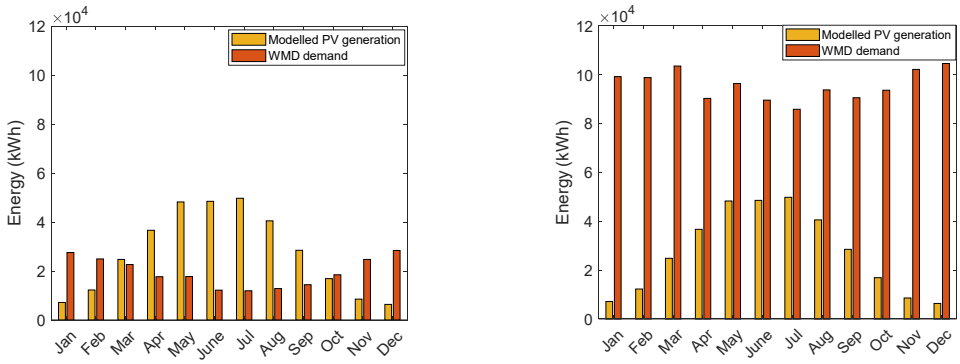

Figure 3. Monthly modelled PV solar energy generation and energy consumption at the WMD: (**a**) with a conventional RCV fleet; (**b**) with an eRCV fleet.

The monthly energy values shown in Figure 3b, when the fleet is assumed to be electric, correspond to the total energy consumed by both the depot and the fleet of 19 eRCVs. When the WMD has a diesel-powered fleet (Figure 3a), the energy consumption reflected in the graph corresponds only to the energy demand by the depot. This follows a seasonal trend, with a higher energy consumption over the winter months, and a decreased energy consumption over the summer months. This seasonal trend is not as pronounced once the fleet is electrified, and there are a few peaks throughout the year. Examining the months of January, April, June and October, the seasonal fluctuation in energy demand is still visible to a lesser extent. Some months, such as March, May and August, peak against this pattern. These peaks are actually linked to the number of days that the fleet is operating. For example, in February, the fleet operates for 20 days, Monday through Friday.

However, in March this increases to 23 operational days. This increase in energy demand by the fleet hides any seasonal fluctuation in energy demand by the depot in those months.

2.5. Energy Management Algorithm (EMA)

In order to assess the impact on costs when a company electrifies the fleet having a PV installation on site and a BESS, as in scenario 2 and scenario 3, two different energy management algorithms (EMA) have been modelled.

Scenario 2 and scenario 3 are differentiated based on two priorities. On one hand, the algorithm in scenario 2 is set to reduce the dependency on the grid during peak price periods at the expense of upgrading the power connection.

On the other hand, the algorithm in scenario 3 is developed to avoid any power connection upgrade at the expense of possibly incurring excess capacity charges.

Both algorithms have been developed in Matlab Simulink and are run in a simulation time step of one hour. Both algorithms are discussed in the following sections.

2.5.1. The EMA for Scenario 2: Prioritise Consumption from Grid at Lower Network Charges and Electricity Prices

The main objective when developing the EMA for scenario 2 was to minimise the cost of the electricity bought from the grid, by prioritising the use of PV solar energy whenever possible. The EMA for scenario 2 connects the system formed by the PV installation, the BESS, the eRCV fleet, and the depot with the grid (as shown previously in Figure 1b).

The depot is assumed to have rooftop PV panels installed and a BESS (with a round trip efficiency of 90% [52]). The energy demand of the depot and the eRCV fleet is covered, firstly by solar energy, secondly by energy stored in the BESS, and lastly by the grid. If there is a PV surplus of solar energy after the total energy demand at the depot has been met, the PV surplus of solar energy is stored in the BESS for later use. A detailed diagram of the algorithm developed for scenario 2 can be seen in Figure 4.

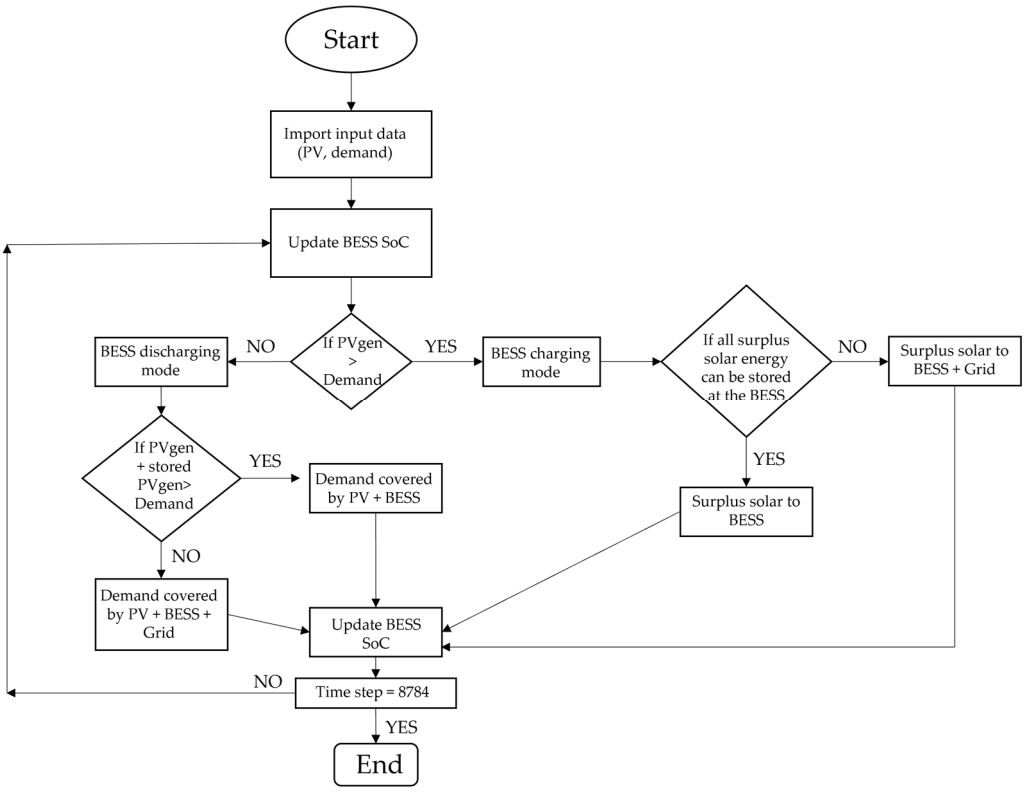

Figure 4. Flow chart of the energy management algorithm developed for scenario 2.

In the algorithm, some constraints have been considered. The battery cannot be charged and discharged within the same hourly time step (t), and it will only operate within the selected state of charge (SoC) range (Equation (17)). SoC_{min} and SoC_{max} are assumed to be 20% and 90% of the total battery capacity, respectively. The selected SoC limits do not reflect any specific equipment but have been chosen as a reasonable range for a typical battery system operation [53].

$$SoC_{min} \leq SoC_{(t)} \leq SoC_{max} \quad (17)$$

The battery will have a constraint for charging and discharging at a maximum power of $2C_{BESS}$ (Equation (18)), where C_{BESS} is the capacity of the battery. Self discharge of the battery is assumed to be negligible. This is consistent with the advice given on numerous Lithium-based cell datasheets, and is meant to avoid rapid cell degradation, to this end operation beyond 2C is not advised.

$$\text{BESS max.power}[\text{kW}] = 2 \cdot C_{BESS}. \quad (18)$$

As it can be seen from Figure 4, the BESS is charged exclusively from the PV installation. The algorithm is run 8784 times as this corresponds to the total number of hour time steps per year. The BESS is modelled assuming that any voltage or current change is achievable with changes in SoC [27]. The SoC is the most frequent parameter used to evaluate the energy status of the battery [53]. According to Byrne et al. [54], this type of model is the best choice when the aim is to perform a technoeconomic analysis and operate in the range of minutes to hours. Yang et al. [27] and Rosewater et al. [53] defined the charging/discharging process of the battery as in Equation (19):

$$C_{BESS} \cdot \frac{\partial SoC}{\partial t} = BESS_{rteff} \cdot {P_{BESS(t)}}^{+} + {P_{BESS(t)}}^{-}, \quad (19)$$

where $BESS_{rteff}$ is the battery round trip efficiency, $\frac{\partial SoC}{\partial t}$ is the rate of change of SoC and ${P_{BESS(t)}}^{+}$,${P_{BESS(t)}}^{-}$ are the charging/discharging power of the BESS, respectively.

When the algorithm ends, the energy into the BESS must be the same as the energy out of the BESS (Equation (20)):

$$BESS_{in} = BESS_{out}. \quad (20)$$

Only when the PV solar energy generation is higher than the WMD and eRCV fleet energy demand is the BESS charged. The surplus solar energy stored in the BESS will also depend on the available capacity in the battery at the time step.

On the other hand, the battery is discharged when there is not enough PV solar energy to meet the energy demand of both the WMD and the eRCV fleet charging. When the BESS is discharged to the minimum SoC, the BESS cannot be further discharged. If the energy demand has not been covered, the grid is then required to support the energy demand from the WMD and the eRCV fleet.

Based on the increase of the peak energy demand when the eRCV fleet is adopted, the EMA for scenario 2 ensures that the system never surpass the peak grid power capacity. This, however, then requires a network upgrade of the grid power connection from 0.15 MW to 0.6 MW.

2.5.2. The EMA for Scenario 3: Avoid the Upgrade of Power Connection Capacity

The main objective when developing the EMA for scenario 3 was to avoid any possible power connection capacity upgrade associated with the switch from a conventional fleet to an electric one. For that purpose, the algorithm utilises a BESS that is charged not only from PV solar energy but also from the grid. The EMA connects the system formed by the PV installation, the BESS, the EV fleet, and the depot with the grid (as shown previously in Figure 1c).

For the development of the algorithm, the BESS constraints used correspond to the same constraints introduced for the EMA developed for scenario 2 (see Equation (17) to Equation (20)). However, a new constraint is set for the EMA created for scenario 3, based on the power connection capacity ($Power_{capacity}$). The constraint is applied when the BESS is charged from the grid. The power required from the grid ($Power_{(t)}$) to charge the BESS cannot be higher than the power connection capacity (Equation (21)).

$$Power_{(t)} < Power_{capacity} \tag{21}$$

Assuming the site cannot upgrade the grid power connection network, the power connection capacity contracted at the site has to be the same as it was before switching the fleet to electric, 0.15 MW. This is conducted at the expense of storing energy from the grid, even during higher price periods as required.

2.6. System Cost Analysis

The economic analysis of the study is performed considering the three scenarios described previously in Table 1: scenario 1, scenario 2, and scenario 3. The cost analysis for scenario 1med at grid power connection capacities of both 0.15 MW and 0.6 MW to facilitate the comparison with scenario 3 and scenario 2, respectively.

The total costs for each scenario have been calculated considering the costs of energy from the grid (E_c), network costs (N_c), cost of the BESS ($BESS_c$), cost of the PV installation (PV_c), and the revenue obtained from the sale of surplus solar energy (Rev_c) following Equation (22).

$$\text{Total costs over system lifetime} = E_c + N_c + BESS_c + PV_c - Rev_c. \tag{22}$$

The purchase cost of the eRCV fleet as well as the costs of the charging installation are not considered for this study. All the scenarios analysed assumed the fleet at the WMD is already electric and therefore the costs are out of scope for the study, and any new investment would be related to the PV and BESS acquisition and installation. Next, each cost is explained.

2.6.1. Cost of Energy (E_c)

The cost of energy refers to the cost of electricity purchased from the grid and is calculated following Equation (23).

$$E_c(£/\text{year}) = \frac{\text{Electricity price}\left(\frac{p}{kWh}\right) \cdot \text{Energy consumption (kWh)}}{100p/£}. \tag{23}$$

The electricity price paid at the WMD was not available for the period of interest and had to be assumed based on market data available from the UK government.

Since 2021, there has been a sharp increase in electricity prices, with global gas prices and wholesale electricity prices quadrupling within the last year. For the WMD, the cost of electricity has been estimated considering the average electricity price in the non-domestic sector published by BEIS [55]. BEIS publishes average quarterly and annual electricity prices based on two surveys conducted across energy suppliers and non-domestic consumers. The depot in this study is in the 'small consumption' band, according to the classification from BEIS. For this band, the electricity price rose by 63% to 25 p/kWh between Q3 2021 and Q3 2022.

Predictions point to a continuous price increase over winter. Unfortunately, the available data for the non-domestic sector has not been updated since Q3 2022, just before the Ofgem price cap came into effect in the UK (1 October–31 December 2022). Since then, the Ofgem price cap has been updated twice. Thus, the change for electricity prices in non-domestic consumers has been extrapolated from the percentage change corresponding to each Ofgem price cap. From the most recent published report for domestic energy prices,

the price cap increased by 80% from April 2022 to October 2022 [56] and 20% from October 2022 to January 2023 [57].

In Figure 5, the electricity prices for the non-domestic sector are shown. These correspond to the small consumption band and include the published prices (purple column) and the extrapolated prices (orange column). The electricity price for Q4 2022 (37.80 p/kWh) was assumed to be 80% higher than the price in Q2 2022 (21.04 p/kWh). In Q1 2023, a further 20% increase was applied to estimate the electricity price (i.e., 45.40 p/kWh).

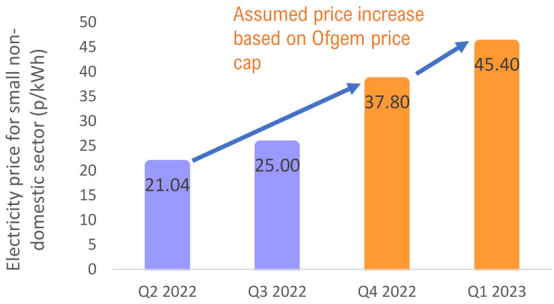

Figure 5. Assumed electricity price for small non-domestic sector from October 2022.

Based on the volatility of prices and continuous increases, the value assumed to be the average price corresponding to Q1 2023 has been considered for this study (i.e., 45.4 p/kWh).

For the WMD, it has been assumed that the company has a variable tariff contract, so the electricity price varies every hour. In order to show a difference in hourly electricity prices, the study has used variations in wholesale electricity prices found on the Nord Pool website for the UK, to create a price profile throughout a typical day [58]. Nord Pool is in the framework of EU Regulation on Wholesale Energy Market Integrity and Transparency for power trading across Europe. As an example, Figure 6 shows the price profile for one day of the year. There are two peak times when the electricity cost is at its highest value (between 6 a.m. and 10 a.m. and 4 p.m.–8 p.m.).

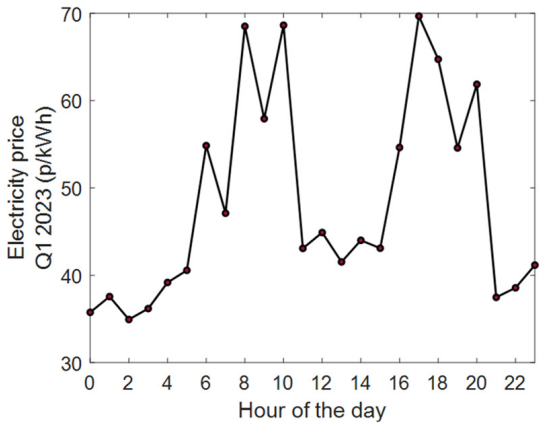

Figure 6. Simulated electricity prices for one day of the year (from 00:00 h to 23:00 h) for the WMD.

2.6.2. Network Charges (N_c)

These refer to the contracted power connection capacity costs and the use of the network distribution system that is charged by the energy supplier. The total network cost (N_c) is the addition of capacity cost (C_c) that exceeded capacity cost (ExC_c), fixed cost (F_c) and consumption band cost ($Consmp_c$) (Equation (24)).

$$N_c = C_c + ExC_c + F_c + Consmp_c \quad (24)$$

Capacity cost is associated with the contracted power connection capacity. If the power connection capacity is exceeded, additional costs will be incurred (i.e., exceeded capacity costs). This is the case in scenario 1 when the power connection capacity is held at 0.15 MW, despite the increase in energy demand due to the electrification of the fleet. The consumption band cost is the price paid for using the network at certain hours over the day and is divided into three different bands:

- The amber band rate is charged between 07:00 h–16:00 h and 19:00 h–21:00.
- The red band rate spans from 16:00 h to 19:00 h.
- The green band rate is from 00:00 h to 07:00 h and from 21:00 h to 24:00 h.

For the WMD, the network charges were selected based on the price from the Western Power Distribution Network in the UK for an LV Site-Specific Band 1 [59]. The network charges are itemised in Table 2.

Table 2. Network charges for the WMD.

Network Charges	Price	Unit of Measure
Capacity charge	2.91	p/kVA/day
Exceeded capacity charge	5.73	p/kVA/day
Fixed charge	297	p/day
Consumption band charge		
Amber band	0.737	p/kWh
Red band	4.301	
Green band	0.054	

The capacity cost, C_c is calculated in Equation (25):

$$C_c(£/\text{year}) = \frac{\frac{\text{Power}_{\text{capacity}}(\text{kW})}{\text{PF}\left(\frac{\text{kW}}{\text{kVA}}\right)} \cdot \frac{\text{Capacity charge}\frac{\text{p}}{\text{kVA}}}{\text{day}} \cdot 365 \text{ days}}{100 \text{ p}/£}. \quad (25)$$

PF is the power factor. For this study, a value of 0.9 has been selected. The annual C_c for each scenario studied can be seen in Table 3.

Table 3. Annual capacity charge for each scenario studied.

	Capacity Cost (£/Year)	
	$\text{Power}_{\text{capacity}}$: 0.15 MW	**$\text{Power}_{\text{capacity}}$: 0.6 MW**
Scenario 1	1770	7081
Scenario 2		7081
Scenario 3	1770	

The total exceeded capacity cost (ExC_c) is calculated as the sum of the excess power capacity multiplied by the exceeded capacity charge each day following Equation (26).

$$ExC_c(£/\text{year}) = \sum_{i=1}^{n} \left(\frac{\left(\frac{\text{Excess power}_{\text{capacity}}(\text{kW})}{\text{PF}\left(\frac{\text{kW}}{\text{kVA}}\right)} \right)_i \cdot \frac{\text{Exceeded capacity charge}\frac{\text{p}}{\text{kVA}}}{\text{day}}}{100\frac{\text{p}}{£}} \right) \quad (26)$$

The fixed costs (F_c) per year are obtained applying Equation (27):

$$F_c\left(\frac{£}{\text{year}}\right) = \frac{\text{Fixed charge}\left(\frac{\text{p}}{\text{day}}\right)}{100\frac{\text{p}}{£}} \cdot 365\text{days}. \quad (27)$$

Finally, consumption band costs ($Consmp_c$) are calculated considering the energy consumption at each band time multiplied by the corresponding band charge as follows (Equation (28)):

$$Consmp_c\left(\frac{£}{year}\right) = \frac{\text{Energy consumption(kWh)}\cdot\text{consumption band charge}\left(\frac{p}{kWh}\right)}{100\frac{p}{£}}. \quad (28)$$

Additionally, the installation costs incurred when the power connection capacity is upgraded are also considered within the scope of this study. According to Energy UK [60], for an upgrade of between 200 kVA and 1000 kVA, the approximate connection costs would be between GBP 4500 and GBP 75,000. Assuming the required power connection capacity would need to increase from 150 kW to 600 kW (i.e., approximately 667 kVA considering a PF of 0.9) for scenario 1 and scenario 2, the assumed network upgrade cost for this study has been obtained by interpolation. The cost assumed is GBP 45,740 [60].

2.6.3. Cost of BESS

For the cost of the BESS, a capital cost of GBP 254/kWh [61] and GBP 2.5/kWh-year in Operation and Maintenance (O and M) costs [62] have been used.

The BESS capital costs are obtained using Equation (29):

$$BESS_{Cc}(£) = C_{BESS}\ (MWh)\cdot\frac{1000\ kWh}{1\ MWh}\cdot 254\frac{£}{kWh}. \quad (29)$$

The O and M cost of the BESS has been calculated in Equation (30).

$$BESS_{OMc}(£) = C_{BESS}\ (MWh)\cdot\frac{1000\ kWh}{1\ MWh}\cdot 2.5\frac{£}{kWh\ per\ year}\cdot\text{BESS lifetime (years)}. \quad (30)$$

BESS lifetime has been assumed to be 15 years [61,62]. In Table 4, the total cost of the BESS ($BESS_c$) has been calculated for each BESS capacity (C_{BESS}) as the addition of $BESS_{Cc}$ and $BESS_{OMc}$.

Table 4. Total cost of BESS for a lifetime of 15 years.

BESS Capacity (MWh)	Capital Cost (£)	O&M Cost (£)	Total Cost in 15 Years (£)
0.05	12,700	1875	14,575
0.1	25,400	3750	29,150
0.5	127,000	18,750	145,750
1	254,000	37,500	291,500
5	1,270,000	187,500	1,457,500
10	2,540,000	375,000	2,915,000

2.6.4. Cost of PV Panels

For the PV installation, it has been assumed a PV panel capital cost equal to £1.25/W_{DC} and O and M cost equal to GBP 17.92/kWp-year [63].

The PV panel capital costs are obtained using Equation (31):

$$PV_{Cc}(£) = \text{Number of PV panels}\cdot\text{PV panel power output (W)}\cdot 1.25\frac{£}{W_{DC}} \quad (31)$$

The O and M cost of the PV installation has been calculated in Equation (32).

$$PV_{OMc}(£) = \text{Number of PV panels}\cdot\text{PV panel power output (W)}\cdot\frac{1\ kW}{1000\ W}\cdot 17.92\frac{£}{kWp\ per\ year}\cdot\text{PV lifetime (years)} \quad (32)$$

Table 5 shows the total cost for the PV installation (PV_c) considering a lifetime of 15 years, as the addition of PV_{Cc} and PV_{OMc}.

Table 5. Total cost of PV installation for a lifetime of 15 years.

Number of PV Panels	PV Panel Power Output, STC (W)	PV System Size (MW)	Capital Cost (£)	O and M Costs (£)	Total Cost in 15 Years (£)
1864	270	0.5	629,100	135,282	764,382

2.6.5. Revenue from the Sale of PV Surplus Solar Energy

For the WMD, it is assumed that the surplus solar energy that cannot be stored is sold back to the grid, and this generates an annual revenue that is considered in the total costs (Equation (33)). For this study, a sale price of 5 pence per kWh has been used [64].

$$\text{Rev}_c(£/\text{year}) = \frac{\text{Sale price}\left(\frac{\text{p}}{\text{kWh}}\right) \cdot \text{surplus solar energy(kWh)}}{100\ \text{p}/£} \quad (33)$$

3. Results

3.1. Economic Impact of Introducing PV Panels and a BESS on Site to Reduce the Consumption from the Grid at Higher Electricity and Network Prices; Comparison between Scenario 1 and Scenario 2

The effect of installing PV panels and a BESS on site can be seen by comparing Figures 7 and 8.

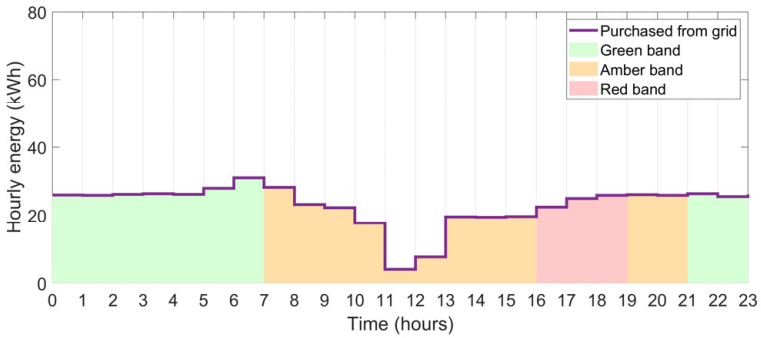

Figure 7. Hourly energy purchased from the grid for a day for scenario 1.

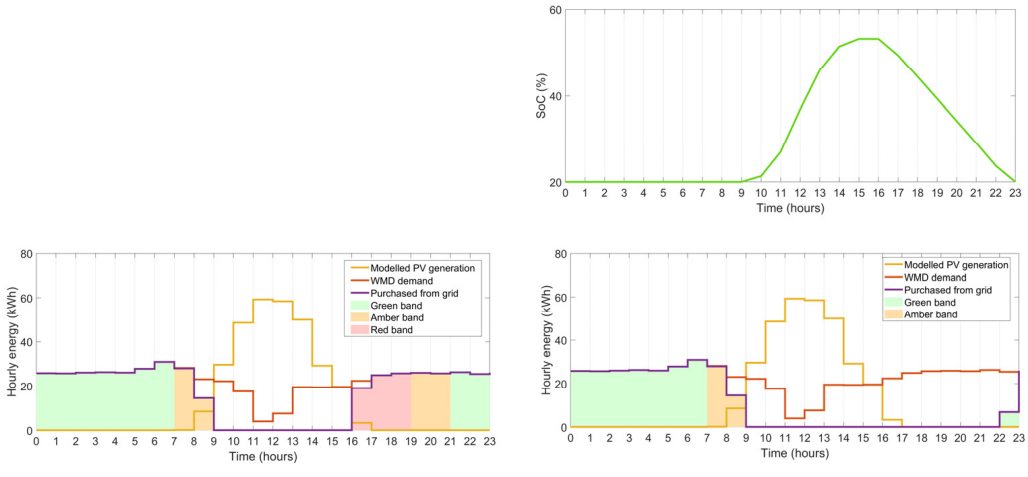

Figure 8. Comparison of the hourly energy consumption from the grid: (**a**) with only PV panels and (**b**) with PV panels and a BESS of 0.5 MWh (scenario 2).

Figure 7 shows hourly values of energy purchased from the grid for scenario 1. For this scenario, the WMD energy demand is entirely covered by the grid because there are no PV panels and BESS installed on site. The coloured areas represent each network consumption band based on the time of the day.

The effects of incorporating PV panels and a BESS into the system (scenario 2) can be seen in Figure 8. Results show hourly energy consumption (i.e., WMD demand), PV solar energy generation (i.e., modelled PV generation), and the energy purchased from the grid for a day during the weekend in February. The WMD demand only reflects the demand from the building as the eRCV fleet does not operate during the weekends. As with Figure 7, the area under the line that represents the energy purchased from the grid (i.e., purple) is coloured in green, amber, and red representing the different consumption time bands. There are areas that are not shaded and implies no energy is being drawn from the grid.

First, to highlight the importance of adding a BESS into the system to reduce the consumption from the grid at higher electricity prices, Figure 8a shows the hourly energy results obtained if only PV panels are installed at the WMD. The consumption from the grid is reduced in comparison with scenario 1 (Figure 7) but only a small portion of the solar energy generated is used directly by the WMD. An important amount of the energy generated is not used instantaneously and is sold back to the grid (i.e., surplus solar energy). When the energy demand is higher than the PV solar energy generation, the grid is required to cover the demand. This occurs in amber and red consumption bands and, therefore, when the electricity cost is at its peak, reducing the economic benefits.

However, when a BESS of capacity equal to 0.5 MWh is installed together with the PV panels (Figure 8b), the surplus solar energy is stored in the BESS to be used at a later time when solar energy is not available to cover the energy demand, and the network costs and electricity prices are at their highest values. This reduces the consumption from the grid further and allows the system to be independent of the grid during the highest electricity price periods, and the highest network consumption band (i.e., red band).

It can be concluded that the BESS plays a key role to maximise the benefits of solar energy generation on site for scenario 2.

The size of the BESS will have a direct impact on the reduction of the dependency of the depot on the grid, and therefore, an impact on energy and network costs. This is shown in Figure 9 using two different BESS capacities for illustration, a 0.5 MWh BESS (Figure 9a) and a 5 MWh BESS (Figure 9b). Figure 9 shows the monthly energy purchased from the grid, the monthly solar energy consumed directly from the PV panels ("consumed from PV"), the monthly solar energy stored at the BESS (stated as "to BESS" in the figure) for later use ("from BESS") and the solar surplus energy sold to the grid ("PV solar surplus").

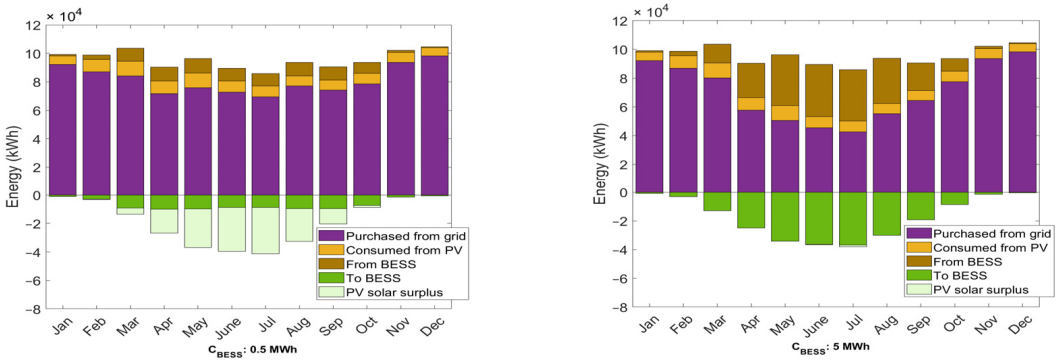

(**a**) (**b**)

Figure 9. Monthly energy simulation results for scenario 2 using a BESS with a capacity of: (**a**) 0.5 MWh and (**b**) 5 MWh. The positive values on each graph represent the energy consumption from the grid, from solar, either directly, or via the BESS. The negative values indicate solar energy generation and energy storage in the BESS.

With a smaller BESS, 0.5 MWh in this case, a lower fraction of the surplus solar energy is stored in the BESS when compared to the surplus solar energy stored with a larger BESS. Here, the BESS is not able to store all the solar energy generated from the PV installation, and a large fraction of the surplus solar energy is sold to the grid, failing to materialise the reduction in grid dependency. A larger BESS, 5 MWh, is able to store most of the solar energy generated for later use, reducing the energy required from the grid. This is especially relevant in summer months when solar energy generation is at its maximum and the limiting factor is the BESS capacity. In winter months, in contrast, the solar generation decreases, and an increase of the BESS size does not reduce the grid dependency. This will be shown in depth in later in the paper.

The energy demand drawn from the grid at different battery capacities can be seen in Figure 10, on an annual basis. For the purpose of the analysis, Figure 10 also includes the results obtained for scenario 1 (No PV or BESS). As the BESS capacity increases, the energy consumed from the grid decreases. This is shown by the decreased purple line in the graph.

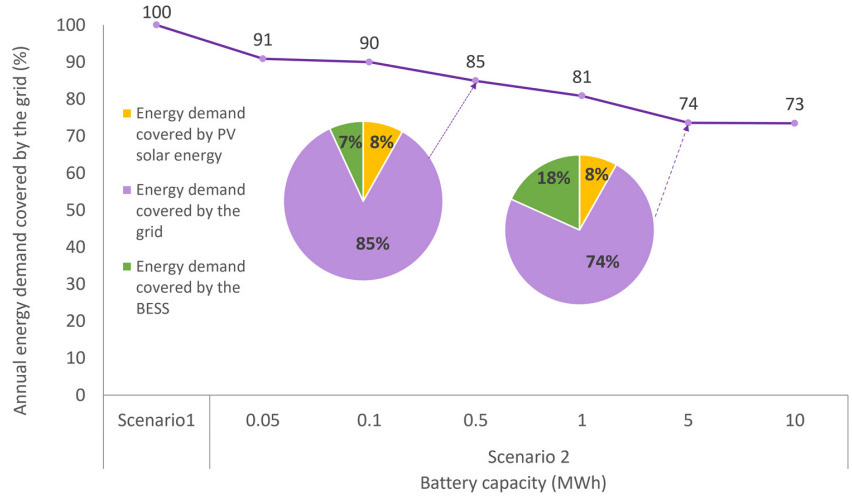

Figure 10. Energy demand covered by the grid for scenario 1 and scenario 2 (purple line), and the breakdown of energy demand covered by the grid, by direct PV generation and by the solar via the BESS for C_{BESS} of 0.5 MWh and 5 MWh as examples (pie charts).

A detailed breakdown is shown for the two BESS analysed before, 0.5 MWh and 5 MWh. At 0.5 MWh, the energy demand from the grid is lowered by 15%. The energy demand is covered as follows: 85% of the energy demand is covered by the grid, 8% is covered directly by the PV generation, and a further 7% is covered by the excess solar energy stored in the BESS. With a BESS of 5 MWh, the energy demand from the grid is lowered by 26% and is broken down into 74% of demand covered by the grid, 8% directly from PV generation, and 18% from solar energy stored in the BESS. For a BESS with a capacity of 10 MWh, a 27% reduction in grid supply is possible.

The hourly energy simulation results for scenario 2 can be seen in Figure 11 for a week in February (Figure 11a) and in July (Figure 11b) for a BESS of 5 MWh.

The BESS SoC can be seen at the top of Figure 11 (green line). In the middle, the energy consumption from the eRCV fleet is shown with a blue line. At the bottom of Figure 11, hourly values of modelled solar energy generation (yellow), WMD energy demand (orange), and energy purchased from the grid (purple) are shown. Hour 0 corresponds to the hour after the 00:00 h on Saturday morning, and the last value (i.e., 23:00 h) corresponds to the last hour of the following Friday night. As can be seen, the eRCV fleet is charged from Monday to Friday, commensurate with the usage patterns discussed previously.

Considering Figure 11a as an example of a week in winter, it can be seen that the energy to cover the eRCV's demand comes entirely from the grid. The benefits of having local PV generation installed and a BESS are minimised when compared to other seasons (i.e., Figure 11b) due to significantly less PV generation in winter.

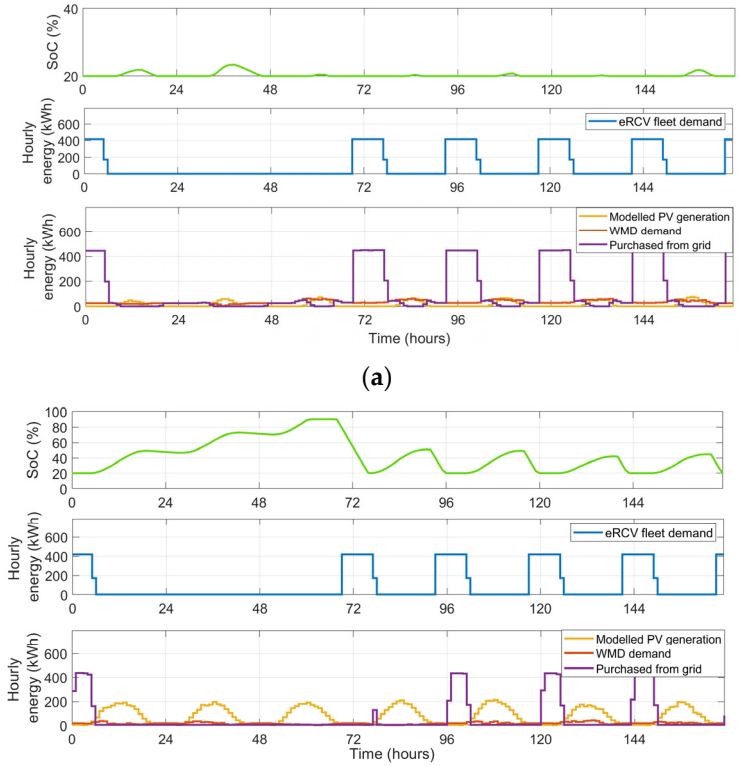

Figure 11. Hourly energy distribution for scenario 2 with a BESS capacity of 5 MWh in a week in (**a**); February and (**b**) July.

However, in summer (Figure 11b), consumption from the grid is reduced significantly, for both the WMD building and the eRCV fleet. During the weekend, the WMD is totally independent from the grid, and due to storing surplus solar energy, the BESS becomes fully charged. Here then, the BESS has stored enough energy to charge part of the fleet at night. On Mondays, the fleet is almost completely charged using the energy stored in the BESS from the weekend PV generation.

The lifetime costs for scenario 1 and for scenario 2 at different BESS capacities have been calculated as shown in Figure 12. The total costs are itemised by network costs, cost of energy, cost of BESS, and cost of PV panels. The revenue from the sale of any surplus solar energy for scenario 2 has been subtracted from the cost of energy.

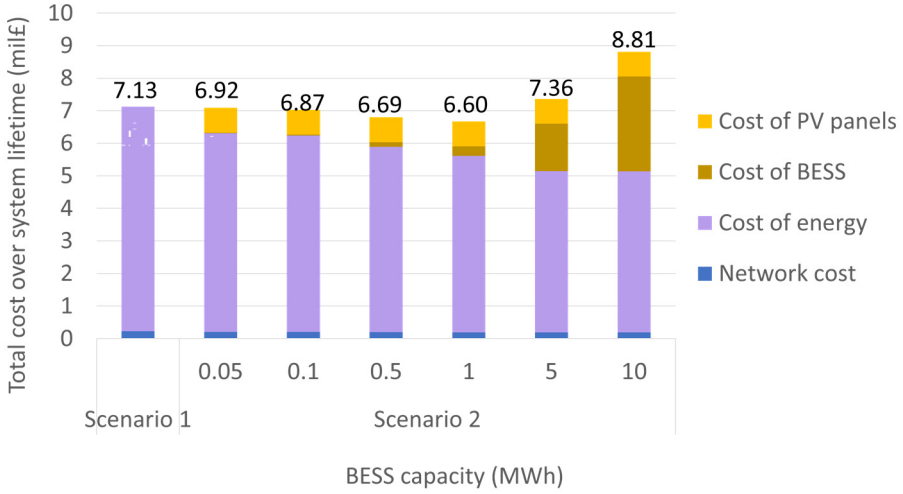

Figure 12. Total cost over system lifetime for scenario 1 and scenario 2.

From the figure, the larger the BESS capacity, the lower the cost of energy. The introduction of a BESS and PV generation would be justified for the purpose of reducing the cost of energy and dependency on the grid. However, when all amortised costs are included (i.e., cost of BESS, cost of PV panels), some battery capacities cease to be economic as a method for annual electricity cost reduction, when compared with scenario 1.

The scenario that reduces the total costs over the system lifetime the most corresponds to scenario 2 with BESS of 1 MWh of capacity. When compared with scenario 1, the total cost reduction over the system lifetime is GBP 530,000.

The system costs for scenario 1 and scenario 2 (itemised at different battery capacities) can be seen in detail in Table 6.

Table 6. System cost at different battery capacities (C_{BESS}) for scenario 1 and scenario 2.

Power Connection Capacity (MW)	Scenarios		Cost of Energy per Year (£)	Surplus Solar Energy Revenue per Year (£)	BESS Capital Cost (£)	BESS O and M Cost (£)	PV Capital Cost (£)	PV O and M Cost (£)	Network Cost over System Lifetime (£)	Total Cost over System Lifetime (mil£)
0.6	Scenario 1		460,405	0	0	0	0	0	222,443	7.13
	Scenario 2 (MWh)	0.05	407,211	11,111	12,700	1875	629,100	135,282	203,362	6.92
		0.1	402,385	10,558	25,400	3750			200,510	6.87
		0.5	379,530	7332	127,000	18,750			194,168	6.69
		1	361,592	4719	254,000	37,500			191,882	6.60
		5	329,997	76	1,270,000	187,500			191,205	7.36
		10	329,479	0	2,540,000	375,000			191,194	8.81

The cost of energy, especially for smaller BESS's, has the most significant influence on the total costs (i.e., between 88% and 56%). For batteries with higher capacities (i.e., 5 MWh), between 20% and 33% of the total cost over the system lifetime comes from the cost of the BESS (i.e., BESS capital cost and BESS O and M cost).

The network cost over the system lifetime is also presented in Table 6 as an addition of all associated costs; capacity cost, fixed cost, cost of network upgrade, and consumption band cost. Exceeded capacity costs are not included because the capacity connection is not exceeded for scenario 2, nor for scenario 1 in this particular case.

As can be seen in Table 6, the network cost decreases as the BESS increases, the highest costs are for scenario 1, and the lowest are for scenario 2 with a BESS of 10 MWh. Network cost is reduced due to the reduction in network consumption costs as shown in Figure 13.

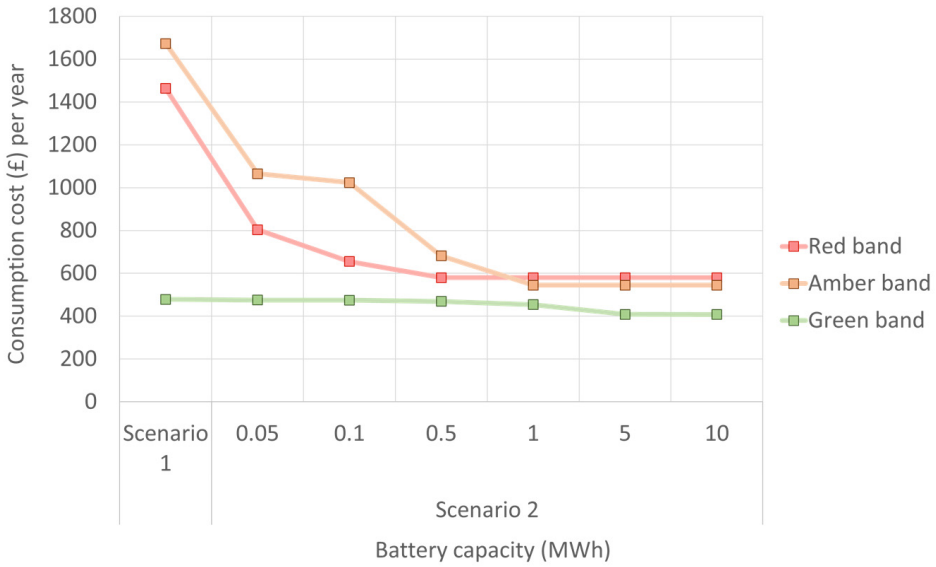

Figure 13. Network consumption cost per year for scenario 1 and scenario 2.

Figure 13 shows the network consumption cost per year at each consumption band for scenario 1 and scenario 2 for different BESS capacities.

The difference in red consumption band costs between scenario 1 and scenario 2 for a BESS capacity of 0.05 MWh is significant. The costs associated with the red band consumption decreases by 43%. For BESS bigger than 0.5 MWh, the cost for the red consumption band is no longer reduced and remains constant at 57%. Most of the reduction within the red band is achieved in summer, when there is enough stored solar energy at the BESS to be used by the system during the red band period, eliminating the need for grid energy in this period. In the winter, there is insufficient PV generation to reduce the red band consumption irrespective of the BESS size.

The costs linked to the amber band also decrease in scenario 2, when compared to scenario 1. Compared to the results obtained for the red band, the costs linked to the amber band can be reduced further for a BESS larger than 0.5 MWh. This is because the amber band takes place later in the day than the red band, so the maximum reduction is achieved with a larger BESS capable of supplying the system with stored excess solar energy for a longer period.

This can be seen for the costs associated with the green band, which is only reduced with a BESS over 1 MWh, because those are the ones capable of storing enough excess solar energy to cover the demand at the beginning of the evening period when the green band is active.

Overall, based on the analysis performed for scenario 1 and scenario 2, it can be concluded that the installation of PV panels and BESS could benefit the economics of a logistics or commercial company when a fleet is electrified and consequently, the energy demand on site proportionately increases.

The algorithm applied in scenario 2 successfully achieves the objective set to reduce the consumption from the grid during higher electricity and network price periods as shown. Here, the total costs over the system lifetime are reduced approximately by GBP 530,000 when PV panels and a BESS of 1 MWh are installed when compared to scenario 1.

Next, the study examines the outcomes for scenario 3 for comparison with scenario 1. Due to the constraint set on the algorithm developed for scenario 3 (the power capacity connection on the WMD when the fleet is electrified cannot be upgraded and the grid connection remains at 0.15 MW), and in order to successfully compare this with scenario 1, the power connection for scenario 1 is also assumed to remain at 0.15 MW.

3.2. Economic Impact of Introducing PV Panels and BESS on Site to Avoid the Upgrade of the Grid Power Connection When the Fleet Is Electrified; Comparison between Scenario 1 and Scenario 3

This section aims to examine one of the barriers that logistics and commercial companies face when they wish to electrify their fleet. That is, a significant increase in energy demand on site, with a constrained grid power connection.

To meet the aim of the section, first, the results obtained from the simulation are analysed. Then, scenario 3 results are compared to scenario 1. From this, the objective to determine the relevance of having PV panels and BESS installed on site under the circumstances described can be met. At the end of the section, all the scenarios studied are compared and discussed further.

The hourly distribution of energy for scenario 3 can be seen in Figure 14 for a week in February (Figure 14a) and for a week in July (Figure 14b). The BESS capacity used in the simulation corresponds to 5 MWh, as before. In the figure, the SoC of the BESS is plotted at the top (green colour), below is the hourly energy consumption from the eRCV fleet (blue line) and at the bottom, the hourly modelled PV generation, the WMD energy demand, and the energy purchased from the grid. Again, the first point of Figure 14 corresponds to a Saturday at 00:00 h, and the last one corresponds to a Friday at 23:00 h.

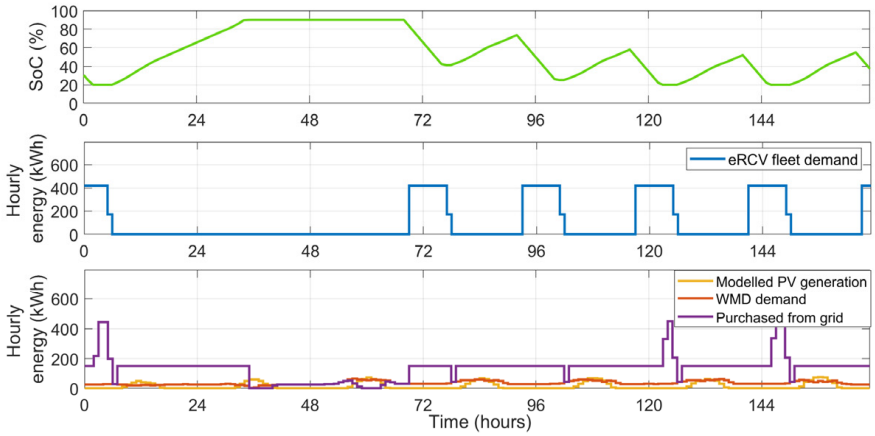

(**a**)

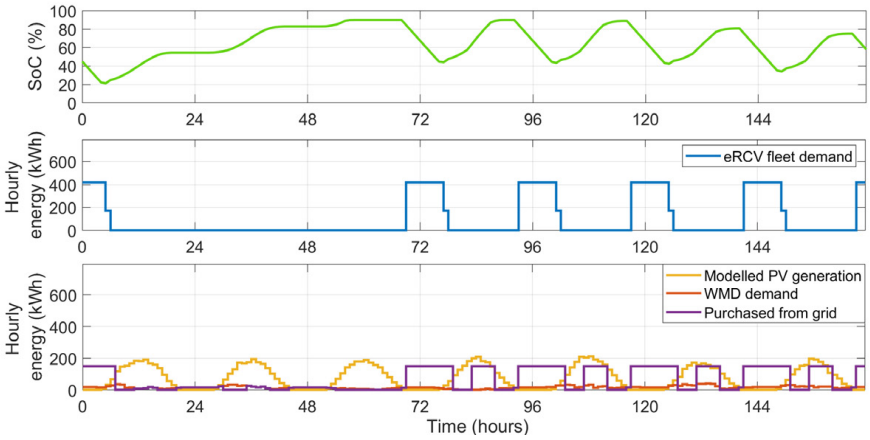

(**b**)

Figure 14. Hourly energy distribution for scenario 3 with a BESS capacity of 5 MWh in a week in (**a**) February and (**b**) July.

On initial inspection, it can be seen that the BESS with 5 MWh capacity is not able to keep the power capacity connection under the initial constraint (i.e., 0.15 MW). This is shown in Figure 14a based on the hourly energy purchased from the grid (purple line).

Here, this happens in three out of seven days in the week. During winter months, the BESS is fully charged on weekends (when the eRCV fleet does not operate) from the grid due to the lower PV generation at this time of the year. This allows the system to avoid exceeding the power connection capacity during the first days of the week (i.e., Monday to Wednesday); however, for the rest of the week, the BESS is not large enough to prevent the power connection capacity from being exceeded in order to successfully charge the eRCV fleet.

In summer (Figure 14b), the system is less dependent on the grid to charge the BESS, and more importantly, the BESS is capable of avoiding exceeding the power connection capacity contracted with the grid network. At this time of the year, PV solar energy generation is at its highest, and it maximises the potential of having PV panels and a BESS installed.

Considering that the constraint set for the algorithm created for scenario 3 has not been met with a BESS of 5 MWh, a larger BESS of 10 MWh was investigated for the simulation, the results obtained can be seen in Figure 15.

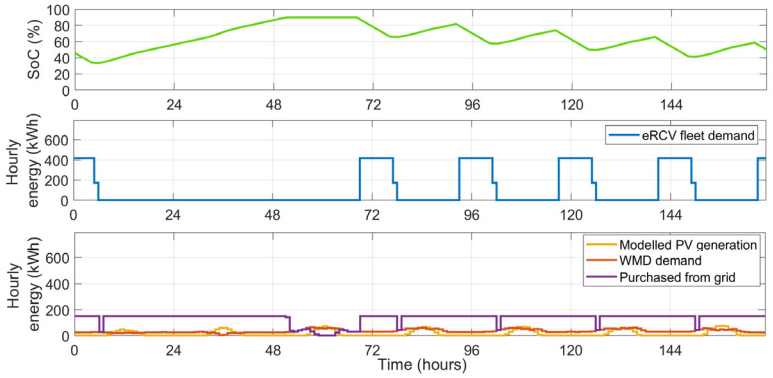

(**a**)

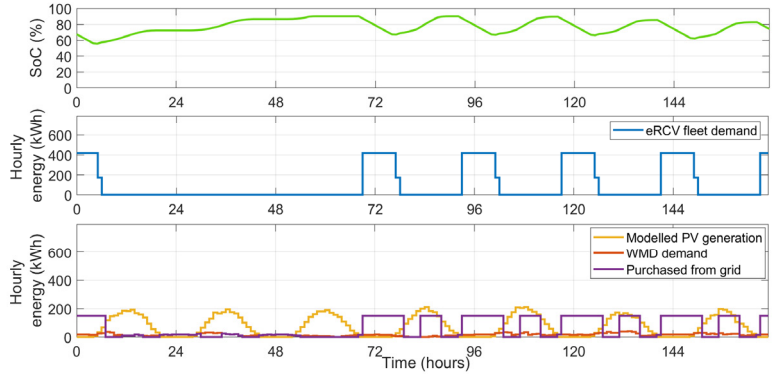

(**b**)

Figure 15. Hourly energy distribution for scenario 3 with a BESS capacity of 10 MWh in a week in (**a**) February and (**b**) July.

Here, with a 10 MWh BESS, the system can keep the power connection capacity within the contracted rating both in winter (Figure 15a) and summer (Figure 15b).

In winter (Figure 15a), the BESS is fully charged during the weekend and stores a higher amount of energy when compared to the smaller BESS, enough to provide energy to the eRCV fleet through the week so the power connection does not have to be upgraded. The BESS is fully charged on Monday and discharged to almost of a 20% of its SoC by the following Friday. It is important to consider that the system needs an almost continuous supply from the grid to be able to achieve the objective set in the algorithm. The BESS is almost fully discharged on Saturday morning when the eRCV fleet has been fully recharged over the previous night.

However, in summer (Figure 15b), the BESS starts the week almost fully charged, and it is only discharged to approximately 60% of its capacity by the end of the week.

As seen in Figure 15, the algorithm has some limitations that could be further improved and are considered a future work. For example, the energy purchased from the grid in summer could be optimised considering the BESS is not discharged below 50% SoC. The algorithm is set to receive the energy from the grid at the maximum connection power capacity, but in summer, it can be reduced and by doing so, the cost of energy would also be reduced too. Additionally, simulation results in Figures 14b and 15b reveal that part of the solar energy generation is not used on site. Approximately 10% and 13% of the PV energy generation is sold to the grid with a BESS of 5 MWh and 10 MWh, respectively. As can be seen in both figures, on Monday, when the PV installation starts to generate solar energy, the BESS is almost fully charged and, therefore, the solar energy has to be sold to the grid.

The total cost over the system lifetime has been estimated for scenario 1 and for scenario 3. The results being presented in Table 7.

Table 7. System cost at for scenario 1 and scenario 3 (with a BESS of 10 MWh).

Power Connection Capacity (MW)	Scenarios		Cost of Energy per Year (£)	Surplus Solar Energy Revenue per Year (£)	BESS Capital Cost (£)	BESS O and M Cost (£)	PV Capital Cost (£)	PV O and M Cost (£)	Network Cost over System Lifetime (£)	Total Cost over System Lifetime (mil£)
0.15		Scenario 1	460,405	0	0	0	0	0	908,840	7.81
	Scenario 3	5 MWh	421,791	2098	1,270,000	187,500	629,100	135,282	231,878	8.75
		10 MWh	427,450	1790	2,540,000	375,000			167,849	10.23

As can be seen, the cost of energy is reduced when PV panels and a BESS are installed when compared with scenario 1.

Furthermore, the network costs are also reduced significantly when scenario 3 is compared with scenario 1. In detail, when PV panels and a BESS of 5 MWh or 10 MWh are on site, the network costs are reduced approximately by 75% and 82%. This provides one of the potential benefits of using a BESS for fleet electrification, as it allows the system to increase the energy demand without exceeding the grid connection power capacity and incurring the extra costs associated with that.

For this particular scenario, the only BESS capable of keeping the grid connection power capacity to the original value (i.e., 0.15 MW) is a BESS with a capacity of 10 MWh. However, when all amortised costs are considered, the total cost over the system lifetime increases significantly when the BESS and the PV panels are installed.

3.3. Is It Economically Feasible to Use PV Panels and a BESS for Freight Fleet Electrification?; Comparison between Scenario 1, Scenario 2 and Scenario 3

The total costs over the system lifetime have been compared between scenario 1, considering both grid connection power capacities (i.e., 0.15 MW and 0.6 MW) in scenario 2 and scenario 3. For scenario 2, the BESS considered for the analysis has a capacity of 1 MWh because this is the one that reduces the total costs over the system lifetime the most. For scenario 3, a BESS with a capacity of 10 MWh has been selected for the analysis on account of being the only BESS capable of constraining the grid connection power to within the contracted capacity.

The total costs over the system lifetime for each scenario are compared in Figure 16a. As can be seen, the most feasible option, in terms of total costs, corresponds to scenario 2. This is characterised by having PV panels and a BESS installed on site. The objective behind scenario 2 is to reduce the consumption from the grid during peak price periods, considering that the introduction of the electric fleet increases the electricity demand of the site considerably. From Figure 16a, it is more cost effective to upgrade the power connection than purchase a larger BESS, if connection capacity is not network constrained at the site.

However, if the upgrade of the power connection capacity is not an option for the logistics or commercial company (i.e., 0.15 MW) due to network constraints out of their control, it would still be worth further exploring the potential benefits of introducing PV panels and a larger BESS. This allows the system to meet the increased energy demand without surpassing the grid connection power capacity. If compared with scenario 1 for the same power connection capacity, the benefits of introducing a 10 MWh BESS when the power connection is not upgraded can be seen in the reduction of the excess capacity charge incurred by the site from approximately GBP 0.8 M to zero (Figure 16b). However, economically it would be difficult due to the high cost of the large BESS shown in Figure 16a (scenario 3). Although the cost of energy storage technology has been decreasing over the last decade [65,66] and from [61], cost projections show a further reduction of between 28% and 58% in capital cost by 2030, BESS cost is still a major barrier to these systems.

If the logistics or commercial company has no intention of installing PV panels and a BESS (i.e., scenario 1), the upgrade of the power capacity connection could reduce the total costs over the system lifetime by approximately GBP 680,000 when compared to

incurring network excess capacity charges when the grid connection power capacity is exceeded (Figure 16b).

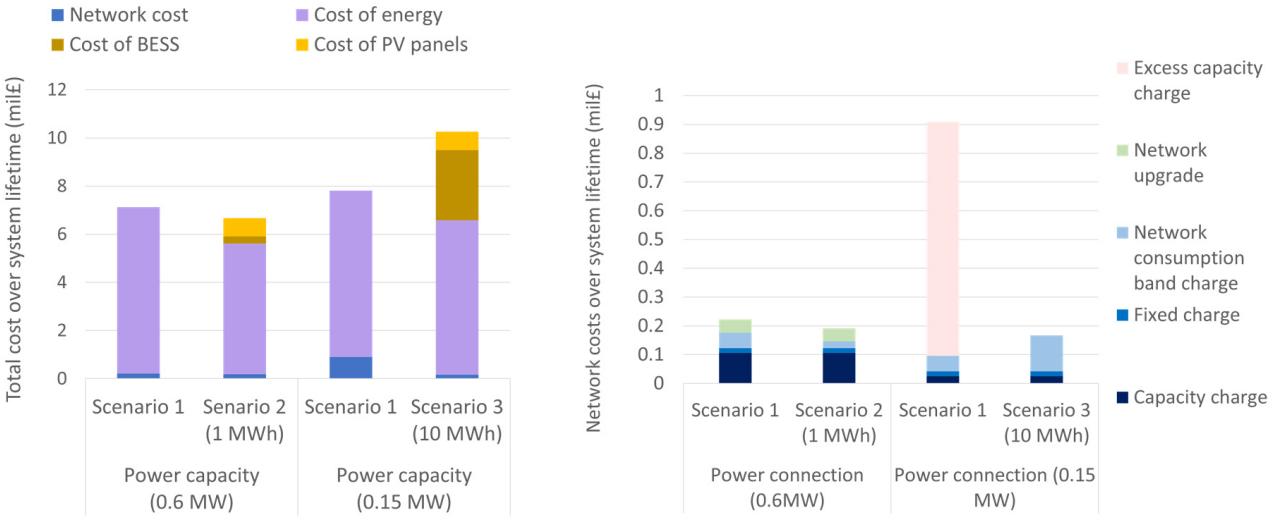

(**a**) (**b**)

Figure 16. Comparison between the three scenarios regarding (**a**) the total cost over the system lifetime and (**b**) the network cost over system lifetime.

4. Conclusions

This study sought to evaluate the impacts on costs when a company electrifies its fleet based on two different priorities: On one hand, avoiding the use of the grid during peak price periods at the expense of upgrading the power connection; On the other hand, avoiding any power connection upgrade at the expense of possibly incurring excess capacity charges. These two priorities aim to represent the real-life challenge that logistics and commercial companies currently face when it comes to fleet electrification. The choice of prioritising one over the other can be influenced by operational requirements or technical constraints.

There are not many references in the literature addressing this challenge, together with renewable energy generation and a BESS. Moreover, publications tend to solve the issue by modifying the charging schedule. However, in real life, this would imply a change in operational requirements and, most of the time, this is not an option.

To fill the gap identified in the literature, this study analyses three different scenarios. For all scenarios, it is assumed that the fleet has been electrified and the energy demand on site has increased significantly. In scenario 1, the logistics or commercial company is not using PV panels and a BESS on site. In contrast, scenario 2 and scenario 3 have PV panels and a BESS installed. However, in scenario 3, the company has a technical constraint, and the power capacity connection cannot be upgraded.

For that purpose, two rule-based energy management algorithms have been developed to manage the energy distribution for scenarios 2 and 3.

As presented, the scenario that reduces costs the most is scenario 2, utilising a 1 MWh BESS. This could reduce the total costs over the system lifetime by GBP 530,000.

It has been demonstrated that having PV panels and a BESS on site reduces the cost of energy for all the scenarios explored, whether the priority is to reduce the grid dependency at peak times or to avoid the upgrade of the power connection.

At times, the upgrade of the power connection is not an option for different reasons outside the customer's control. Under these circumstances, the system incurs an extra cost due to the excess capacity charge if the grid connection power capacity is surpassed. It has been demonstrated that under these circumstances, a BESS with a capacity of 10 MWh allows the system to meet the energy requirements without exceeding the contacted grid

connection power capacity. However, when all amortised costs are included, the use of PV panels and a BESS of the required size cease to be a feasible solution. The cost of the BESS minimises the potential benefits under this scenario. Further improvement is required for the algorithm developed under the grid connection power constraint and forms part of future research. The limitations of the algorithm could be improved by optimising the energy purchased from the grid in summer. During this time, the BESS is not discharged below 50% SoC. The algorithm is set to receive the energy from the grid at the maximum connection power capacity, but in summer, this could be reduced and by doing so, the cost of energy would also be reduced. Additionally, simulation results reveal that part of the PV generation is not used on site, with approximately between 10% and 13% of PV energy generation being sold to the grid when a BESS of 5 MWh and 10 MWh are installed, respectively. Finally, battery degradation is going to be considered in the economic cost analysis for future research.

Author Contributions: Conceptualization, M.N.M., E.E.F.B. and D.A.S.; methodology, M.N.M. and D.A.S.; validation, M.N.M., E.E.F.B. and D.A.S.; formal analysis, M.N.M.; data curation, E.E.F.B. and D.A.S.; writing—original draft preparation, M.N.M.; writing—review and editing, M.N.M., E.E.F.B. and D.A.S.; visualization, M.N.M.; supervision, E.E.F.B. and D.A.S.; project administration, E.E.F.B. and D.A.S.; funding acquisition, E.E.F.B. and D.A.S. All authors have read and agreed to the published version of the manuscript.

Funding: This research was funded by the Engineering and Physical Sciences Research Council (EPSRC).

Data Availability Statement: The data presented in this study are not publicly available.

Conflicts of Interest: The authors declare no conflict of interest; the funders had no role in the design of the study; in the collection, analyses, or interpretation of data; in the writing of the manuscript; or in the decision to publish the results.

References

1. DfT. Transport and Environment Statistics. 2022. Available online: https://www.gov.uk/government/statistics/transport-and-environment-statistics-2022/transport-and-environment-statistics-2022 (accessed on 18 November 2022).
2. Martins-Turner, K.; Grahle, A.; Nagel, K.; Göhlich, D. Electrification of Urban Freight Transport—A Case Study of the Food Retailing Industry. *Procedia Comput. Sci.* **2020**, *170*, 757–763. [CrossRef]
3. Jahn, R.M.; Syré, A.; Grahle, A.; Martins-Turner, K.; Göhlich, D. Methodology for Determining Charging Strategies for Freight Traffic Vehicles based on Traffic Simulation Results. *Procedia Comput. Sci.* **2021**, *184*, 656–661. [CrossRef]
4. Schmid, F.; Taube, L.; Rieck, J.; Behrendt, F. Electrification of Waste Collection Vehicles: Technoeconomic Analysis Based on an Energy Demand Simulation Using Real-Life Operational Data. *IEEE Trans. Transp. Electrif.* **2021**, *7*, 604–615. [CrossRef]
5. Toniato, E.; Mehta, P.; Marinkovic, S.; Tiefenbeck, V. Peak load minimization of an e-bus depot: Impacts of user-set conditions in optimization algorithms. *Energy Inform.* **2021**, *4*, 23. [CrossRef]
6. Anosike, A.; Loomes, H.; Udokporo, C.K.; Garza-Reyes, J.A. Exploring the challenges of electric vehicle adoption in final mile parcel delivery. *Int. J. Logist. Res. Appl.* **2021**, *1*, 25. [CrossRef]
7. Juan, A.A.; Mendez, C.A.; Faulin, J.; De Armas, J.; Grasman, S.E. Electric vehicles in logistics and transportation: A survey on emerging environmental, strategic, and operational challenges. *Energies* **2016**, *9*, 86. [CrossRef]
8. Quak, H.; Nesterova, N.; Van Rooijen, T.; Dong, Y. Zero Emission City Logistics: Current Practices in Freight Electromobility and Feasibility in the Near Future. *Transp. Res. Procedia* **2016**, *14*, 1506–1515. [CrossRef]
9. Morganti, E.; Browne, M. Technical and operational obstacles to the adoption of electric vans in France and the UK: An operator perspective. *Transp. Policy* **2018**, *63*, 90–97. [CrossRef]
10. Berkeley, N.; Bailey, D.; Jones, A.; Jarvis, D. Assessing the transition towards Battery Electric Vehicles: A Multi-Level Perspective on drivers of, and barriers to, take up. *Transp. Res. Part A Policy Pract.* **2017**, *106*, 320–332. [CrossRef]
11. Guo, F.; Yang, J.; Lu, J. The battery charging station location problem: Impact of users' range anxiety and distance convenience. *Transp. Res. Part E Logist. Transp. Rev.* **2018**, *114*, 1–18. [CrossRef]
12. De Socio, M. Plugging into Amazon's Fleet Electrification Strategy. GreenBiz 2020. Available online: https://www.greenbiz.com/article/plugging-amazons-fleet-electrification-strategy (accessed on 14 April 2022).
13. Amazon. Shipment Zero. 2019. Available online: https://sustainability.aboutamazon.com/environment/sustainable-operations/shipment-zero (accessed on 14 April 2022).
14. Crozier, C.; Morstyn, T.; McCulloch, M. The opportunity for smart charging to mitigate the impact of electric vehicles on transmission and distribution systems. *Appl. Energy* **2020**, *268*, 114973. [CrossRef]

15. Chen, F.; Chen, Z.; Dong, H.; Yin, Z.; Wang, Y.; Liu, J. Research on the Influence of Electric Vehicle Multi-Factor Charging Load on a Regional Power Grid. In Proceedings of the 2018 10th International Conference on Measuring Technology and Mechatronics Automation, Changsha, China, 10–11 February 2018; Institute of Electrical and Electronics Engineers Inc.: Piscataway, NJ, USA, 2018; pp. 163–166. [CrossRef]
16. UPS&GreenBiz. Curve Ahead: The Future of Commercial Fleet Electrification. 2018. Available online: https://www.greenbiz.com/report/curve-ahead-future-commercial-fleet-electrification (accessed on 28 September 2022).
17. Pietracho, R.; Wenge, C.; Komarnicki, P.; Kasprzyk, L. Multi-Criterial Assessment of Electric Vehicle Integration into the Commercial Sector—A Case Study. *Energies* **2023**, *16*, 462. [CrossRef]
18. Schmidt, M.; Staudt, P.; Weinhardt, C. Decision support and strategies for the electrification of commercial fleets. *Transp. Res. Part D Transp. Environ.* **2021**, *97*, 102894. [CrossRef]
19. Kin, B.; Hopman, M.; Quak, H. Different charging strategies for electric vehicle fleets in urban freight transport. *Sustainability* **2021**, *13*, 13080. [CrossRef]
20. Pelletier, S.; Jabali, O.; Laporte, G. Charge scheduling for electric freight vehicles. *Transp. Res. Part B Methodol.* **2018**, *115*, 246–269. [CrossRef]
21. Nguyen, V.L.; Tran-Quoc, T.; Bacha, S.; Nguyen, B. Charging strategies to minimize the peak load for an electric vehicle fleet. In Proceedings of the IECON 2014—40th Annual Conference of the IEEE Industrial Electronics, Dallas, TX, USA, 29 October–1 November 2014; pp. 3522–3528. [CrossRef]
22. Arango Castellanos, J.D.; Dhanasekaran Velayutha Rajan, H.; Rohde, A.K.; Denhof, D.; Freitag, M. Design and simulation of a control algorithm for peak-load shaving using vehicle to grid technology. *SN Appl. Sci.* **2019**, *1*, 951. [CrossRef]
23. Ioakimidis, C.S.; Thomas, D.; Rycerski, P.; Genikomsakis, K.N. Peak shaving and valley filling of power consumption profile in non-residential buildings using an electric vehicle parking lot. *Energy* **2018**, *148*, 148–158. [CrossRef]
24. Wenge, C.; Pietracho, R.; Balischewski, S.; Arendarski, B.; Lombardi, P.; Komarnicki, P.; Kasprzyk, L. Multi usage applications of li-ion battery storage in a large photovoltaic plant: A practical experience. *Energies* **2020**, *13*, 4590. [CrossRef]
25. Houbbadi, A.; Trigui, R.; Pelissier, S.; Redondo-Iglesias, E.; Bouton, T. A quadratic programming based optimisation to manage electric bus fleet charging. *Int. J. Electr. Hybrid Veh.* **2019**, *11*, 289–307. [CrossRef]
26. Tang, W.; Zhang, Y.J. A Model Predictive Control Approach for Low-Complexity Electric Vehicle Charging Scheduling: Optimality and Scalability. *IEEE Trans. Power Syst.* **2017**, *32*, 1050–1063. [CrossRef]
27. Yang, Y.; Bremner, S.; Menictas, C.; Kay, M. Modelling and optimal energy management for battery energy storage systems in renewable energy systems: A review. *Renew. Sustain. Energy Rev.* **2022**, *167*, 112671. [CrossRef]
28. Anglani, N.; Oriti, G.; Colombini, M. Optimized energy management system to reduce fuel consumption in remote military microgrids. *IEEE Trans. Ind. Appl.* **2017**, *53*, 5777–5785. [CrossRef]
29. Divshali, P.H.; Choi, B.J.; Liang, H. Multi-agent transactive energy management system considering high levels of renewable energy source and electric vehicles. *IET Gener. Transm. Distrib.* **2017**, *11*, 3713–3721. [CrossRef]
30. Alam, M.S.; Arefifar, S.A. Energy Management in Power Distribution Systems: Review, Classification, Limitations and Challenges. *IEEE Access* **2019**, *7*, 92979–93001. [CrossRef]
31. Moradi, H.; Esfahanian, M.; Abtahi, A.; Zilouchian, A. Optimization and energy management of a standalone hybrid microgrid in the presence of battery storage system. *Energy* **2018**, *147*, 226–238. [CrossRef]
32. Betz, J.; Hann, M.; Jager, B.; Lienkamp, M. Evaluation of the Potential of Integrating Battery Electric Vehicles into Commercial Companies on the Basis of Fleet Test Data. In Proceedings of the 2017 IEEE 85th Vehicular Technology Conference (VTC Spring), Sydney, Australia, 4–7 June 2017. [CrossRef]
33. Engelhardt, J.; Zepter, J.M.; Gabderakhmanova, T.; Marinelli, M. Energy management of a multi-battery system for renewable-based high power EV charging. *ETransportation* **2022**, *14*, 100198. [CrossRef]
34. Arfeen, Z.A.; Abdullah, M.P.; Sheikh, U.U.; Siddique, A.; Raheem, A.; Kausar, M. Efficient energy flow criteria of hybrid solar battery packs grid for electric vehicle rapid-charging facility. *Int. J. Ambient. Energy* **2023**. [CrossRef]
35. Gailani, A.; Al-Greer, M.; Short, M.; Crosbie, T. Degradation cost analysis of Li-Ion batteries in the capacity market with different degradation models. *Electronics* **2020**, *9*, 90. [CrossRef]
36. García-Miguel, P.L.C.; Alonso-Martínez, J.; Arnaltes Gómez, S.; García Plaza, M.; Asensio, A.P. A Review on the Degradation Implementation for the Operation of Battery Energy Storage Systems. *Batteries* **2022**, *8*, 110. [CrossRef]
37. Bukar, A.L.; Tan, C.W.; Yiew, L.K.; Ayop, R.; Tan, W.S. A rule-based energy management scheme for long-term optimal capacity planning of grid-independent microgrid optimized by multi-objective grasshopper optimization algorithm. *Energy Convers. Manag.* **2020**, *221*, 113161. [CrossRef]
38. Coraddu, A.; Gil, A.; Akhmetov, B.; Yang, L.; Romagnoli, A.; Ritari, A.; Huotari, J.; Tammi, K. Energy storage on ships. In *Sustainable Energy Systems on Ships: Novel Technologies for Low Carbon Shipping*; Elsevier: Amsterdam, The Netherlands, 2022; pp. 197–232. [CrossRef]
39. Jafari, M.; Malekjamshidi, Z. Optimal energy management of a residential-based hybrid renewable energy system using rule-based real-time control and 2D dynamic programming optimization method. *Renew. Energy* **2020**, *146*, 254–266. [CrossRef]
40. Zhao, R.; Stincescu, T.; Ballantyne, E.E.F.; Stone, D.A. Sustainable city: Energy usage prediction method for electrified refuse collection vehicles. *Smart Cities* **2020**, *3*, 1100–1116. [CrossRef]
41. CEDA. CEDA Archive. 2017. Available online: https://www.ceda.ac.uk/services/ceda-archive/ (accessed on 16 March 2021).

42. Met Office. MIDAS Open: UK hourly solar radiation data, v202007. *Cent Environ. Data Anal.* **2020**. [CrossRef]
43. Nunez Munoz, M.; Ballantyne, E.E.F.; Stone, D.A. Development and evaluation of empirical models for the estimation of hourly horizontal diffuse solar irradiance in the United Kingdom. *Energy* **2022**, *241*, 122820. [CrossRef]
44. Kittler, R.; Darula, S. Determination of time and sun position system. *Sol. Energy* **2013**, *93*, 72–79. [CrossRef]
45. Soulayman, S. Comments on solar azimuth angle. *Renew. Energy* **2018**, *123*, 294–300. [CrossRef]
46. Sunter, M. MIDAS Data User Guide for UK Land Observations. 2021. Available online: http://cedadocs.ceda.ac.uk/id/eprint/1492 (accessed on 25 September 2021).
47. Brownson, J.R.S. Sun-Earth Geometry. In *Solar Energy Conversion Systems*; Elsevier Science & Technology: Saint Louis, MI, USA, 2014.
48. Duffie, J.A.; Beckman, W.A. Solar Radiation. In *Solar Engineering of Thermal Processes*, 4th ed.; John Wiley & Sons: Hoboken, NJ, USA, 2013.
49. Demain, C.; Journée, M.; Bertrand, C. Evaluation of different models to estimate the global solar radiation on inclined surfaces. *Renew. Energy* **2013**, *50*, 710–721. [CrossRef]
50. Shukla, K.N.; Rangnekar, S.; Sudhakar, K. Comparative study of isotropic and anisotropic sky models to estimate solar radiation incident on tilted surface: A case study for Bhopal, India. *Energy Rep.* **2015**, *1*, 96–103. [CrossRef]
51. Reindl, D.T.; Beckman, W.A.; Duffie, J.A. Evaluation of hourly tilted surface radiation models. *Sol. Energy* **1990**, *45*, 9–17. [CrossRef]
52. Das, C.K.; Bass, O.; Kothapalli, G.; Mahmoud, T.S.; Habibi, D. Overview of energy storage systems in distribution networks: Placement, sizing, operation, and power quality. *Renew. Sustain. Energy Rev.* **2018**, *91*, 1205–1230. [CrossRef]
53. Rosewater, D.M.; Copp, D.A.; Nguyen, T.A.; Byrne, R.H.; Santoso, S. Battery Energy Storage Models for Optimal Control. *IEEE Access* **2019**, *7*, 178357–178391. [CrossRef]
54. Byrne, R.H.; Nguyen, T.A.; Copp, D.A.; Chalamala, B.R.; Gyuk, I. Energy Management and Optimization Methods for Grid Energy Storage Systems. *IEEE Access* **2017**, *6*, 13231–13260. [CrossRef]
55. BEIS. Gas and Electricity Prices in the Non-Domestic Sector—GOV.UK. 2022. Available online: https://www.gov.uk/government/statistical-data-sets/gas-and-electricity-prices-in-the-non-domestic-sector (accessed on 1 June 2022).
56. Bolton, P.; Stewart, I. Domestic energy prices—House of Commons. 2022. Available online: https://commonslibrary.parliament.uk/research-briefings/cbp-9491/ (accessed on 11 January 2023).
57. Ofgem. Latest Energy Price Cap Announced by Ofgem | Ofgem. 2022. Available online: https://www.ofgem.gov.uk/publications/latest-energy-price-cap-announced-ofgem (accessed on 11 January 2023).
58. Nord Pool. Market Data | Nord Pool UK. 2022. Available online: https://www.nordpoolgroup.com/en/ (accessed on 1 June 2022).
59. Western Power Distribution. Western Power Distribution—Charging Statements. 2022. Available online: https://www.westernpower.co.uk/our-network/use-of-system-charges/charging-statements (accessed on 1 June 2022).
60. Energy UK. *Connecting Your Fleet: A Guide for Businesses in Greater London*; Energy UK: London, UK, 2020.
61. Cole, W.; Frazier, A.W.; Augistine, C. *Cost Projections for Utility—Scale Battery Storage: 2021 Update*; National Renewable Energy Lab. (NREL): Golden, CO, USA, 2021.
62. Kebede, A.A.; Kalogiannis, T.; Van Mierlo, J.; Berecibar, M. A comprehensive review of stationary energy storage devices for large scale renewable energy sources grid integration. *Renew. Sustain. Energy Rev.* **2022**, *159*, 112213. [CrossRef]
63. Ramasamy, V.; Feldman, D.; Desai, J.; Margolis, R. *U.S. Solar Photovoltaic System and Energy Storage Cost Benchmarks: Q1 2021*; National Renewable Energy Lab. (NREL): Golden, CO, USA, 2021.
64. Reid, G.; Wynn, G. The future of solar power in the United Kingdom. *Energies* **2015**, *8*, 7818–7832. [CrossRef]
65. Kichou, S.; Markvart, T.; Wolf, P.; Silvestre, S.; Chouder, A. A simple and effective methodology for sizing electrical energy storage (EES) systems based on energy balance. *J. Energy Storage* **2022**, *49*, 104085. [CrossRef]
66. Zhu, K.; Li, X.; Campana, P.E.; Li, H.; Yan, J. Techno-economic feasibility of integrating energy storage systems in refrigerated warehouses. *Appl. Energy* **2018**, *216*, 348–357. [CrossRef]